PLOS COMPLEX SYSTEMS

RESEARCH ARTICLE

Informing pandemic intervention strategies through coupled contact tracing and network node prioritization

Adithya Narayanan[1], **Sarah Muldoon**[1,2], **Matthew Jehrio**[3], **Rachael Hageman Blair**[1,4]*

1 Institute for Artificial Intelligence and Data Science, University at Buffalo, Buffalo, New York, United States of America, **2** Department of Mathematics, University at Buffalo, Buffalo, New York, United States of America, **3** University of Rochester Medical Center, Rochester, New York, United States of America, **4** Department of Biostatistics, University at Buffalo, Buffalo, New York, United States of America

* hageman@buffalo.edu

OPEN ACCESS

Citation: Narayanan A, Muldoon S, Jehrio M, Blair RH (2025) Informing pandemic intervention strategies through coupled contact tracing and network node prioritization. PLOS Complex Syst 2(6): e0000041. https://doi.org/10.1371/journal.pcsy.0000041

Editor: Claus Kadelka, Iowa State University, UNITED STATES OF AMERICA

Received: February 07, 2024

Accepted: March 20, 2025

Published: June 2, 2025

Peer Review History: PLOS recognizes the benefits of transparency in the peer review process; therefore, we enable the publication of all of the content of peer review and author responses alongside final, published articles. The editorial history of this article is available here: https://doi.org/10.1371/journal.pcsy.0000041

Data availability statement: The code to reproduce simulations can be found on: https://doi.org/10.5281/zenodo.15127912.

Abstract

SARS-CoV-2 has highlighted the challenges of social intervention measures for disease control, which are difficult to implement and highly disruptive to modern society. Simulation models have demonstrated the efficacy of primary and secondary tracing at SARS-CoV-2 disease control but at the cost of quarantining large proportions of the population. This paper develops novel tracing strategies that harness node (individual) influence in a social association network for contact-tracing approaches to disease control. The overarching assumption is that an individual's potential to spread disease can be modeled by their ability to propagate influence through a network. Models of idea and influence propagation have been widely studied in the context of social networks but have limited application to disease models. The PRIoritization and Complex Elucidation (PRINCE) algorithm is leveraged to estimate an individual node's influence score that reflects their ability to propagate disease based on network connectivity. In this study, we propose novel augmented tracing strategies that leverage a node's influence to assist with targeted tracing in its 1-hop and 2-hop neighborhoods: i) pseudo-secondary tracing (tracing and quarantining the immediate contacts and the influential contacts of contacts of an infectious symptomatic individual) and ii) selective secondary tracing (tracing and quarantining the influential immediate contacts, and influential contacts of contacts of an infectious symptomatic individual). Contagion dynamics on simulated and real-world networks, benchmarked with existing strategies, demonstrate that our novel strategies mitigate societal disruption by lowering the maximum number of people quarantined concurrently while also assisting the ease of on-ground deployment by reducing the number of individuals to be traced for every infectious individual detected when compared with the most effective existing tracing strategy. Novel approaches of this type that embed network influence into pandemic control provide an opportunity for disease control that ultimately lessens the disruption to society.

Funding: This work was supported by the National Science Foundation (DMS 1312250 to RHB). The funders had no role in study design, data collection and analysis, decision to publish, or preparation of the manuscript.

Competing interests: The authors have declared that no competing interests exist.

Author summary

Contact tracing to effect quarantines is a common method to stem disease dispersion, of which primary tracing (tracing the immediate contacts of an identified case) and secondary tracing (tracing the immediate contacts and the contacts of contacts of an identified case) are the most employed strategies. Due to the rigorous nature of quarantining 2-hop neighborhoods, the latter is extremely effective in outbreak control, but yields a high number of individuals placed in quarantines simultaneously. This strategy is also rigorous to deploy, owing to the vast number of individuals to be traced for every infection. Adopting a network-based approach to modeling social associations, we identify the most influential nodes in a network - the super spreaders in a community - and harness this information to develop novel tracing strategies that are more effective than primary tracing (reduced cumulative and concurrent infections, isolations, and quarantines). Compared to secondary tracing, these strategies offer a significant reduction in the maximum number of people quarantined concurrently with a minor increase in concurrent infections and isolations- however, with the additional benefit of tracing fewer individuals for every identified case and cumulatively, in most scenarios.

Introduction

Measures to attenuate disease dispersion are fundamental to pandemic control. Apart from isolating infectious and symptomatic individuals, contact tracing and quarantines are important non-pharmaceutical interventions in outbreak control, especially for diseases that spread rapidly [1]. However, intervention strategies that separate an individual from societal functions and human contact for prolonged durations have multiple pitfalls owing to their disruptive nature.

The ongoing SARS-CoV-2 pandemic, with its rapid increases in case counts and a lack of medical and socio-logistical resources to stem outbreaks, demonstrated the need to deploy measures that minimize disease transmission. Isolations, quarantines, and lockdowns formed the pillars of such interventions but were accompanied by the friction they caused to societal functions. Apart from their contributions to a personal loss of work and income, such measures also contribute adversely to the mental health of individuals undergoing these practices [2]. Sustained loss of income, lack of logistical support, and psychological tensors have been identified as factors influencing a lack of desire to follow such measures [3] and poor compliance with intervention strategies with several of these obstacles has also been noted [4]. Minimizing these ill effects of intervention strategies is an essential need.

Networks that depict associations that can lead to disease transmission have been used widely to understand and model outbreak dynamics [5]. Studies have sought to better understand contagion dynamics and the effect of intervention strategies on small [6] and large [7] populations. The novel insights offered by a network-based approach to studying epidemics have allowed for augmentations such as the usage of evolving networks [8] and inculcation of metadata such as intensity of contact between nodes [6].

Recently, Firth et al. [6] used a network-based approach to simulate and analyze disease transmissions and the efficacy of tracing strategies such as primary tracing (tracing the immediate contacts of a symptomatic individual to effect preventive quarantines) and secondary tracing (includes immediate contacts and contacts of contacts in its purview). In their simulations, secondary tracing reduced outbreak size the most, but at the cost of, at times, quarantining almost half the population. While aiding outbreak control, quarantining large

proportions of the population over time is highly disruptive. In a rapidly spreading pandemic, such as SARS-CoV-2, a brisk rise in cases can lead to vast numbers of individuals that need to be traced simultaneously - making on-ground deployment laborious and expensive, rising in magnitude from primary to secondary tracing. When juxtaposed with their socio-economic impact on an individual due to loss of work and income and the economic impact of tracing-driven intervention strategies manifesting as human hours and resource costs to trace contacts of symptomatic individuals, the efficacy of tracing-driven intervention strategies fuels the need to find workable alternatives.

A potential alternative to alleviate societal disruption is to leverage the social structure of a population. In communicable diseases, person-to-person contact is the means of transmission. The term *super-spreader* has been defined differently across research studies and diseases but broadly relates to an individual with a higher than average chance to infect many [9]. For COVID-19, it has been estimated that 10% of individuals are responsible for 80% of total infections [10]. A recent review highlighted that social participation offers more than average transmission opportunities for super-spreaders in COVID-19, and in the initial stage of the pandemic, case studies have underscored the need to identify and isolate super-spreaders [11]. The major contribution of this work is the use of network structure to inform pandemic response in a way that balances societal disruption with disease control by engaging network-informed prioritization to identify and isolate high-potential disease spreaders. Informing tracing strategies with node influence aims to control or extinguish a pandemic while lessening the societal impact of tracing and easing the burden of tracing.

This paper develops novel augmented tracing strategies that embed network influence scores estimated using the Prioritization and Complex Elucidation (PRINCE) algorithm [12]. Modified tracing strategies aim to prioritize influential nodes in a social association network in an infectious node's 1st and 2nd hop neighborhoods to cushion the tradeoff between outbreak control and societal disruption. Existing and augmented tracing strategies were benchmarked on outbreaks simulated on randomly generated and real-world networks that characterize social associations. Results show that pseudo-secondary tracing and selective secondary tracing lower the mean maximum number of individuals in quarantine concurrently compared to primary or secondary tracing strategies. They also yield lower cumulative metrics of infections, isolations, and quarantines compared to primary tracing and lower the mean maximum number of infectious and isolated individuals concurrently. Although secondary tracing leads to lower infections and isolations cumulatively on average, pseudo-secondary and selective secondary tracing, offer a balanced solution by mitigating a key implementation barrier of having to trace a higher number of individuals for every identified infectious individual while also preventing mass quarantines in comparison, thereby assisting the reduced disruption to routine.

Materials and methods

Social associations as networks

Modeling social interactions is key to understanding communicable disease transmission in a population. Networks (graphs) that depict associations between individuals naturally represent such an ecosystem. In the scope of disease transmission, individuals concurrently sharing a physical space which can function as a conduit to infection is regarded as a social association. In this setting, the nodes in the network represent individuals, and the edges depict social association. Since diseases transmitted through physical interactions can be transmitted by either individual sharing an edge to the other, in this work, it is assumed that the associations are undirected.

In disease networks, individuals are represented by a single node, and a node's neighborhood (connected nodes) represents the corresponding individual's immediate contacts. This simplistic 1-hop neighborhood is leveraged for primary tracing, and 2-hop neighborhoods are leveraged for secondary tracing [6]. Factors such as susceptibility, hygiene, workplace exposure, and living conditions can affect transmission. However, for simplicity, it is assumed that transmission across edges is equally likely and is reflected by unweighted edges.

Node prioritization

Based on a network's structure, nodes may contribute differently to disease spread. The ability of a node to spread infection through a network is inextricably linked to its connection to other nodes in the network. A node's connectivity can be characterized using measures such as its centralities and clustering coefficients [13–16]. This work focuses on a measure of *influence* that reflects a node's ability to propagate information through the network. In the disease networks, we assume the information reflects disease. Influence scores for each node are computed using the PRIoritizatioN and Complex Elucidation (PRINCE) algorithm [12]. Mathematically, we define an undirected network, $G \in \mathbf{R}^{n\times n}$, as a symmetric binary adjacency matrix $g(i,j) = g(j,i) = 1$ if nodes i and j are connected, and $g(i,j) = g(j,i) = 0$ otherwise. An individual cannot infect themselves in an outbreak, and hence, the diagonal elements $g(i,i) = 0$. A normalized form of this matrix, $G' = D^{-1/2}GD^{-1/2}$ is computed, where $D \in \mathbf{R}^{n\times n}$ is a diagonal matrix with entries $d(i,i)$ as the degree of the ith node. The vector of influence scores, $F \in \mathbf{R}^{n\times 1}$ are computed iteratively as follows:

$$F^t = \alpha G' F^{t-1} + (1-\alpha)Y, \tag{1}$$

until convergence, where $Y \in \mathbf{R}^{n\times 1}$ indicates any prior on the scores, which we assume is uniform in our applications [12]. For the scope of this work, we retain a constant alpha of 0.95, however, in the presence of available prior information on node influence, an appropriate alpha must be chosen. The iterative method has been shown to converge to the exact solution [12,17], but offers better computational efficacy with larger networks. Influence scores computed by PRINCE rely on network structure such that a node's scores are guided by the scores of their neighbors. Furthermore, PRINCE anchors itself on balancing centrality-like influence scoring with prior information on a node's influence in a network when available or expertly defined. Notably, alternative methods for computing node influence, such as centrality measures [15], also aim to assign a score of influence to each node in the network. In this work, PRINCE is adopted because of the computational efficiency and convergence properties. However, alternative measures could be easily adopted in this framework.

Intervention strategies

A node with greater influence score catalyzes a greater spread of an outbreak. The following three augmented tracing strategies are designed to leverage influence scores from PRINCE and to target the tracing of such influential nodes. In this work, a node is considered influential if its influence score falls in the top 25% of the influence scores obtained from all the nodes in a network.

- **Selective primary tracing:** Primary tracing involves isolating symptomatic individuals and quarantining their immediate contacts. Selective primary tracing augments primary tracing by quarantining only those immediate contacts who are most influential.

- **Selective secondary tracing:** In selective secondary tracing, we trace and quarantine the influential contacts, and the influential contacts of contacts of a symptomatic node by augmenting secondary tracing which does not account for a node's influence.
- **Pseudo-secondary tracing:** Pseudo-secondary tracing uses features from both primary and secondary tracing and inculcates a tracing approach that is partially guided by influence. In this strategy, we trace and quarantine all the immediate contacts of a symptomatic node, like in primary tracing, but also quarantine the node's influential secondary contacts.

A summarization of tracing features is presented in Table 1. Since selective primary and selective secondary tracing limit the list of nodes to traced based on influence scores, they limit the number of people that can be quarantined concurrently and cumulatively and offers ease of on-ground deployment owing to the reduced tracing efforts. These strategies focus on curbing outbreak spread by aiding the tracing of the most influential nodes in a network. In contrast, pseudo-secondary tracing offers flexibility by allowing for tracing more nodes since it implements a full primary tracing. It also strengthens primary tracing's outbreak control by selectively tracing the influential secondary contacts of a symptomatic individual to assist in bridging the gap between primary tracing and secondary tracing, while offering ease of deployment by limiting the number of secondary contacts to be traced in comparison.

Fig 1 depicts a visual implementation of all five tracing strategies with one infectious individual on a representative network where the size of the nodes depict their influence in the network. When a node exhibits symptoms and is isolated, augmented strategies target influential nodes in their contact tracing process. Selective primary and secondary tracing strategies quarantine fewer individuals than their respective regular counterparts and pseudo-secondary tracing quarantines fewer individuals than secondary tracing while still targeting the influential individuals in the 2-hop neighborhood of an isolated node.

Outbreak simulations on networks

Simulations were performed using generated Erdos-Renyi Networks and Barabasi-Albert Networks. Experiments depicting different outbreaks were also simulated on the Haslemere Network, which [6] used to study contagion dynamics. An overview of each type of network used in the simulations, along with their key characteristics, the number of networks constructed and the number of outbreaks simulated on each network is outlined in Table 2. All the networks considered were unweighted.

The `igraph` package [18] was used to simulate random networks. Briefly, Erdos-Renyi Networks networks [19] are defined by two parameters - the vertex count and the edge

Table 1. Features of contact tracing for existing and augmented intervention strategies.

	Immediate Contacts	Contacts of Contacts	Influential Immediate Contacts	Influential Contacts of Contacts
Primary tracing	✓			
Secondary tracing	✓	✓		
Selective primary tracing			✓	
Selective secondary tracing			✓	✓
Pseudo-secondary tracing	✓			✓

https://doi.org/10.1371/journal.pcsy.0000041.t001

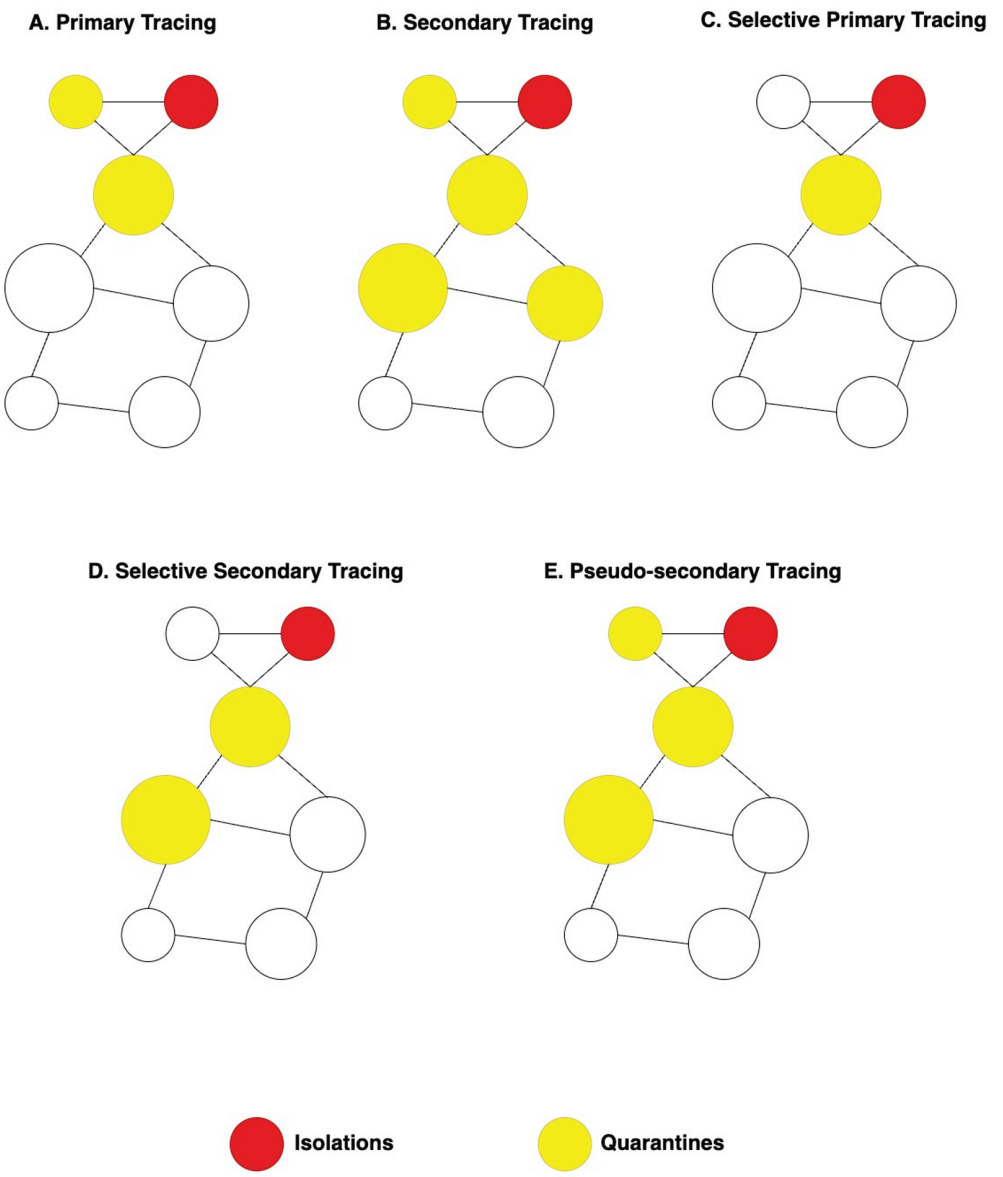

Fig 1. Comparative illustrations of influence-based novel augmented tracing strategies with existing tracing strategies. (A) Primary, (B) Secondary, (C) Selective primary, (D) Selective secondary, and (E) Pseudo-secondary tracing implemented for an infectious node in a network where solid lines depict the edges in the 1-hop and 2-hop neighborhoods of an infectious symptomatic individual who is isolated and dashed lines depict connections to other nodes in the network. Node shaded with a red hue denotes the infectious isolated individual and nodes shaded with a yellow hue denote individuals quarantined based on the choice of tracing strategy with influential individuals in the overall network marked textually.

https://doi.org/10.1371/journal.pcsy.0000041.g001

count. For a given number of nodes, an Erdos-Renyi network is constructed by sampling the predefined number of edges uniformly from all possible dyadic node combinations. As an alternative to using a predefined edge count, a probability of an edge existing between any arbitrary dyad can also be specified. In our simulations, edge counts are used to specify network sizes and networks with 500 nodes, and 1999 edges, are constructed. Barabasi-Albert

Table 2. An overview of network characteristics and their corresponding outbreak simulation load.

Network	(Nodes, Edges)	Type	Number of Networks	Outbreaks per Network
Erdos-Renyi	(500, 1999)	Uniform edge sampling	100	100
Barabasi-Albert	(500, 1990)	Preferential Attachment	100	100
Haslemere	(411, 1257)	Real World – GPS Social Tracking Data based	1	100

https://doi.org/10.1371/journal.pcsy.0000041.t002

Networks [20] model the preferential attachment process. Specifically, beginning with a single node, more nodes and edges are added iteratively such that nodes with more connections tend to develop more edges, exhibiting a rich-get-richer phenomenon. The probability, p_i, of an edge connecting to a node $i \in V$ is given by: $p_i = \frac{d_i}{\sum_{j \in V} d_j}$, where d_i and d_j are the degrees of nodes i and j respectively. Barabasi-Albert networks with 1000 nodes and 3990 edges were also examined to investigate the scalability of these approaches. The Haslemere Network [6] was defined from social interaction data [21]. The network has 468 individuals (nodes) and 1257 social links (edges).

Outbreak simulations on networks were defined using a branching process model [22] implemented in the `COVIDHM` library [6]. A total of 100 Erdos-Renyi and 100 Barabasi-Albert Networks were simulated (Table 2). For each of these networks, 100 unique outbreak setups (starting point of an outbreak). Since the Haslemere Network is predefined, 100 outbreak setups are simulated on this network. Each intervention strategy is applied to each network and outbreak simulation. Each outbreak is initiated by randomly infecting a node in a given network, and outbreak spread is monitored and updated at a day-level granularity. Each outbreak is simulated for a duration of 150 days. On each day, as the infection is transmitted through the network, and each node is labeled as either Susceptible, Infectious, or Recovered. Those with the disease are termed *Infectious* nodes, and in the simulations are considered asymptomatic or symptomatic using Bernoulli Trials where the probability of a node being asymptomatic is set to 0.2 and the rate of a node being able to transmit infection before exhibiting symptoms is also set to 0.2. Symptomatic nodes are isolated, and subsequently, contact tracing based on the strategy deployed during the outbreak is carried out. Recovery time for every symptomatic node is set to 7 days after onset and isolations and quarantines are carried out for 14 days. While a node is symptomatic with a fixed probability, thereby being isolated eventually in infectious, a node being infected and isolated aren't simultaneous processes, with a delay separating the change in status. This change in status in a node being now deemed infected and subsequently isolated can also happen when it was already in quarantine. Each of these changes in status contributes to the trends in concurrent measures of the epidemiological metrics. Any infectious node that is not separated from the population through isolation or quarantine is able to continue disease dispersion in the network. The delay between onset and isolation is modeled using a Weibull distribution with a shape and scale of 1 and 1.4, and the incubation period of infection is also modeled using a Weibull Distribution with a mean of 5.75 days.

Between a pair of contacts, the transmission rate is modeled using the methods leveraged by Firth et al. [6], defined by:

$$\lambda(t, s_i, p_i) = A_{s_i} \int_{t-1}^{t} f(u; \mu_i, \alpha_{p_i}, \omega_{p_i}) du$$

where t is the number of days since a node i was exposed to infection, s_i depicts whether node i is symptomatic (yes/no), and p_i depicts whether the transmission is presymptomatic (yes/no). A_{s_i}, represented in S1 Table, represents the scaling factor for infection transmission, whereas the probability density function $f(u; \mu_i, \alpha_{p_i}, \omega_{p_i})$ models the generation time of infection, and is a skewed normal distribution which relies on the infector's onset time μ_i as its location parameter, and the slant and scale parameters, α_{p_i} and ω_{p_i} rely on whether a node transmits infection pre-symptoms such that $\alpha_{p_i} = -\infty$ for presymptomatic transmissions, and ∞ for post-symptomatic transmissions whereas $\omega_{p_i} = 2$ for presymptomatic transmission, and is set to the onset time for post-symptomatic transmission. With this transmission rate, the simulations leverage $P(t, s_i, p_i) = 1 - e^{-\lambda(t, s_i, p_i)}$ as the probability of an infection between an infector and a susceptible node, t days after the infector's exposure.

A detailed list of the key parameters is given in S1 Table. In each individual outbreak, and for each tracing approach, we measure daily counts of infections, isolations, quarantines and at its conclusion, and the cumulative measures of these three metrics.

Results

Case counts were obtained across all the simulations and grouped by network and tracing strategy. Erdos-Renyi and Barabasi-Albert network simulations yield 10000 simulations for each tracing strategy, stemming from 100 randomly generated networks with 100 outbreaks on each such network, and thereby 10000 observations of every recorded measure. Notably, the Haslemere simulation is a fixed network, yielding only 100 unique simulated outbreaks per tracing strategy on the network.

Fig 2 portrays mean concurrent metrics as a curve of the number of isolated, quarantined, and infectious individuals on the same day across all simulations. Fig 2 is organized by network type (rows) and tracing strategy (columns). The y-axis is kept constant within rows to facilitate direct comparison within networks across tracing strategy. Specifically, the rows represent Erdos-Renyi (Fig 2, A1–A5), Barabasi-Albert (Fig 2, B1–B5), and Haslemere (Fig 2, and the different tracing strategies are represented in the columns: primary tracing (Fig 2, A1–C1), secondary tracing (Fig 2, A2–C2), selective primary tracing (Fig 2, A3–C3), selective secondary tracing (Fig 2, A4–C4) and psuedo-secondary tracing (Fig 2, A5–C5). The cumulative medians and means of infections, isolations, and quarantines are shown in Table 3.

Fig 2A2–C2 demonstrate that secondary tracing consistently yields the lowest maxima of mean concurrent infections and isolations across all networks. However, across every network, we observe a taller peaks in the mean daily number of quarantines when compared with other strategies deployed on the same network type, showcasing this strategy's nature of quarantining a large proportion of people at a single time point.

Secondary tracing also shows low cumulative numbers of mean and median isolations and infections across Erdos-Renyi, Barabasi-Albert, and Haslemere Network simulations (Table 3), which is the lowest across all strategies. Mean quarantines by secondary tracing are always lower than primary tracing regardless of the network. In comparison with pseudo-secondary tracing, this strategy yields lower mean and median quarantines in Erdos-Renyi simulations, but in the Barabasi-Albert and Haslemere simulations, the quarantine metrics are close and comparable.

Primary tracing performs weakly compared to every tracing strategy involving any tracing of secondary contacts. With concurrent quarantines, depicted by Fig 2A1–C1, on the same network type, primary tracing mimics secondary tracing (Fig 2A2–C2) closely, but this is also accompanied by a high peak of concurrent infections and isolations. This trend holds true across every type of network. Only selective primary tracing (Fig 2A3–C3) does worse

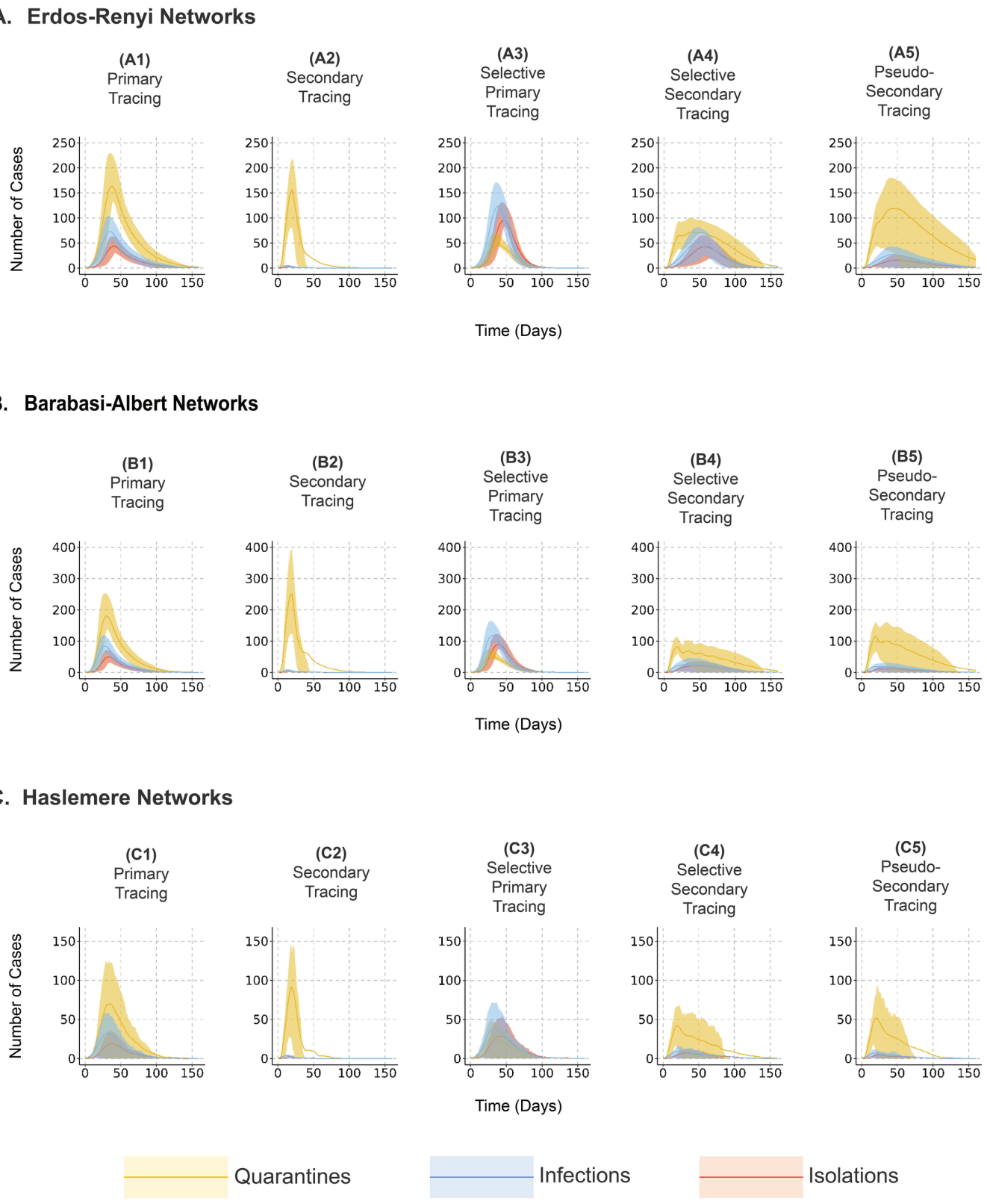

Fig 2. A comparison of the effect of tracing strategies on concurrent quarantines. Concurrent mean isolations, infections, and quarantines with percentile ribbons from outbreak simulations on (A) Erdos-Renyi, (B) Barabasi-Albert, and (C) Haslemere Networks, organized as rows. Columns represent tracing strategies implemented: (A1-C1) Primary, (A2-C2) Secondary, (A3-C3) Selective primary tracing, (A4-C4) Selective secondary, and (A5-C5) Pseudo-secondary tracing. Solid lines depict mean values, with the shaded ribbons depicting the values observed at the 25th and 75th percentiles.

https://doi.org/10.1371/journal.pcsy.0000041.g002

due to its nature of limiting the number of individuals who can be quarantined, eroding the already weak primary tracing methodology. In sharp contrast to secondary tracing, primary and selective primary tracing yield the highest mean and median isolations, infections, and quarantines on any network type across all methods.

Selective secondary tracing caps the number of individuals that can be traced as well, thereby limiting cumulative and concurrent quarantines to a maximum of a quarter of the network's size. However, its targeted nature of tracing high-influence nodes from the first and second-level contacts of a symptomatic individual lends to its efficacy compared to selective primary tracing. Table 3 shows that in Erdos-Renyi simulations, the mean and median cumulative infections and isolations from this strategy are lower than primary tracing while

Table 3. Cumulative median and mean (with ± margin of error for the 95% confidence intervals) of isolations, quarantines, and infections across all simulations, grouped by network type and the intervention strategy deployed.

Erdos-Renyi Graph (500 Nodes, 1999 Edges)	**Medians**		**Isolations**	**Quarantines**	**Infections**
		Primary	234	468	296
		Secondary	4	198	5
		Selective primary	311	121	392
		Selective secondary	230	125	289
		Pseudo-secondary	157	438	198
	Means		**Isolations**	**Quarantines**	**Infections**
		Primary	196.8 ± 1.84	386.8 ± 3.47	248.7 ± 2.32
		Secondary	6.65 ± 0.15	221.2 ± 2.60	8.39 ± 0.20
		Selective primary	260.5 ± 2.33	100.9 ± 0.87	327 ± 2.92
		Selective secondary	184 ± 1.95	104.3 ± 0.78	231 ± 2.45
		Pseudo-secondary	125.1 ± 1.52	339.2 ± 3.42	158.1 ± 1.93
Barabasi-Albert Networks (500 Nodes, 1990 Edges)	**Medians**		**Isolations**	**Quarantines**	**Infections**
		Primary	217	468	275
		Secondary	5	346	6
		Selective primary	290	122	365
		Selective secondary	163	125	205
		Pseudo-secondary	100	366	126
	Means		**Isolations**	**Quarantines**	**Infections**
		Primary	189.6 ± 1.56	403.5 ± 3.17	239.7 ± 1.96
		Secondary	11.95 ± 0.29	317.2 ± 3.12	15.14 ± 0.38
		Selective primary	252.7 ± 1.98	105.7 ± 0.79	317.4 ± 2.48
		Selective secondary	124 ± 1.71	107.7 ± 0.64	155.6 ± 2.15
		Pseudo-secondary	86.24 ± 1.32	287.9 ± 3.03	109 ± 1.67
Haslemere Networks (468 Nodes, 1257 Edges)	**Medians**		**Isolations**	**Quarantines**	**Infections**
		Primary	116.5	300	150
		Secondary	3	102	3
		Selective primary	153	98	190.5
		Selective secondary	8	79.5	11.5
		Pseudo-secondary	6	76.5	6.5
	Means		**Isolations**	**Quarantines**	**Infections**
		Primary	81.34 ± 12.8	193.1 ± 29.5	103.1 ± 16.21
		Secondary	4.86 ± 1.14	124.68 ± 20.06	6.18 ± 20.06
		Selective primary	103.2 ± 16.53	61.47 ± 9.31	130.2 ± 20.9
		Selective secondary	33.66 ± 7.96	63.44 ± 8.00	42.45 ± 10.04
		Pseudo-secondary	21.05 ± 5.29	103.91 ± 17.52	26.39 ± 6.73

https://doi.org/10.1371/journal.pcsy.0000041.t003

keeping mean and median cumulative isolations much lower than pseudo-secondary tracing. In Barabasi-Albert simulations, the performance gap widens between selective secondary and primary tracing, with the former offering significantly lower metrics on all fronts. This difference between tracing strategies is more profound in the Haslemere Simulations. In comparison, pseudo-secondary tracing entails higher median and mean quarantines but lowers infections and isolations across all three types of networks.

However, selective secondary tracing's most salient feature, depicted in Fig 2A4–C4, lies in its ability to maintain a plateaued mean daily quarantine curve regardless of which network it is deployed on. While keeping concurrent quarantines low, it also offers better control over concurrent infections and isolations compared to primary and selective primary tracing. Although secondary (Fig 2A2–C2) and pseudo-secondary (Fig 2A5–C5) tracing strategies offer better control over concurrent infections and isolations across all networks, selective secondary tracing offers comparable performance with the benefit of lower concurrent quarantines.

Pseudo-secondary tracing, in Fig 2A5–C5, exhibits lower mean and median concurrent infections and isolations than all strategies deployed on the same type of network, except secondary tracing. It offers a strong argument in its favor by preventing situations where a vast amount of individuals are quarantined at the same time while also lowering the efforts required for an on-ground deployment of the strategy. Although selective secondary tracing (Fig 2A4–C4) trumps pseudo-secondary tracing on a given type of network when it comes to concurrent quarantine metrics, the latter yields lower concurrent mean isolations and infections consistently. Table 3 shows that across Erdos-Renyi, Barabasi-Albert, and Haslemere simulations, pseudo-secondary tracing offers lower mean and median isolations and infections than all strategies except secondary tracing -while it quarantines more individuals than selective secondary tracing, it does so with an edge in isolation and infection metrics. Simulations with larger Barabasi-Albert networks (1000 nodes) showed a similar phenomenon when comparing across tracing strategies (S2 Table, S1 Fig). Although the magnitude of the cases is notably larger, it is proportional to the network size and the trends are consistent.

The effects of thresholds that designate a node as influential were examined systematically across network types and tracing strategies. Specifically, we simulated outbreaks with the same parameters when the nodes corresponding to the top 10% (S2 Fig) and 20% (S3 Fig) of influence scores are considered influential. In these cases, we observe that with a decrease in the number of nodes considered influential, there is a decrease in the number of nodes quarantined concurrently, which yields an increase in infections and isolations. As the threshold for influential nodes shifts from the top 20% to the top 10%, the differences become more pronounced across all strategies and networks, with a noticeable increase in infections and isolations and a decrease in quarantines. This can be attributed to the significantly lower number of candidates eligible for quarantine, resulting in less resistance to the spread of an outbreak. While considering fewer nodes as influential still produces similar trends in concurrent outbreak metrics, the magnitude of differences varies. In comparison, at 25%, quarantines remain more controlled than with existing strategies, keeping a significant proportion of the network free of quarantine at any given time. Additionally, this approach reduces concurrent infections and isolations more effectively than when a lower proportion of nodes are considered influential.

Discussion

This work introduced prioritization-based contact tracing. The PRINCE algorithm was used to calculate the prioritization scores largely due to its flexibility and scalability [12]. However,

the score calculations can be viewed as modular; alternative prioritization or influence scores could be explored within this tracing framework [23,24]. This work demonstrates that augmented strategies, selective secondary tracing and pseudo-secondary tracing, are viable alternatives that can be employed based on situational needs. While secondary tracing remains the most impactful strategy for keeping infections and isolations low, these strategies offer alternatives that minimize disruptions caused by a large number of people placed in quarantines concurrently or cumulatively while still offering better solutions to infections and isolations than primary tracing. Limited studies have used network measures in disease modeling and control. These include applications in modeling the extent of disease spread [25,26], transmission [27,28], epidemic source detection [29], and targeted resource and immunization allocation [25,30]. To the authors' knowledge, this represents the first study to leverage measures of node influence in contact tracing strategies and ultimately provide a tunable mathematical balance of societal disruption and infection control.

The prioritization-based selective secondary tracing caps the number of people who can be quarantined across the duration of our simulations. This ensures that not more than a quarter of the number of individuals in a network will ever be traced or asked to quarantine. Furthermore, selective secondary tracing also prevents many people from being traced and asked to quarantine at a single point in an outbreak. Pseudo-secondary tracing, on the other hand, also assists with limiting the number of quarantined individuals concurrently. Due to its implementation of full primary tracing as part of its methodology, the number of people traced to quarantine concurrently and cumulatively are observed to be higher than in selective secondary tracing in our experiments. However, pseudo-secondary tracing offers consistently lower cumulative and concurrent infections than selective secondary tracing across the Erdos-Renyi, Barabasi-Albert, and Haslemere Simulations. Selective secondary tracing and pseudo-secondary tracing are viable alternatives depending on the situational need in an outbreak. In a situation where the number of individuals concurrently in quarantine needs to be controlled while minimizing the trade-off of higher infections and isolations, pseudo-secondary tracing comes to the fore, whereas when an outbreak is in a phase where minimizing quarantine metrics is a priority, but a relative increase in infections and isolations is acceptable, selective secondary tracing is a viable alternative.

Due to their prioritization-based nature, selective secondary tracing and pseudo-secondary tracing require less effort to deploy on-ground than secondary tracing on a case-by-case basis. Compared to primary tracing, pseudo-secondary tracing is more laborious but offers significant improvement in all three metrics - isolations, infections, and quarantines- concurrently and cumulatively. Selective secondary tracing, in contrast, requires tracing only a select set of nodes in a network, making tracing efforts simpler. This study focuses on networks structures with differing characteristics but of similar population size of ~ 500 individuals, selective secondary and pseudo-secondary tracing scale robustly to simulations on larger preferential attachment networks with a 1000 individuals and 3990 associations. Additional research is required to assess the scalability of these tracing strategies to larger communities.

A limitation of our simulation models is the required specification of a large number of parameters. Although the model is adaptable to other pandemics, results are sensitive to differences in incubation periods, reproduction numbers, and isolation and quarantine durations. Modeling a wider range of these values and their permutations and potentially accounting for their evolution with time is an important area to explore. Furthermore, this study compartmentalized nodes based on the SIR model [31]. In this work, a node is considered influential if its influence score lies in the top quarter of the influence scores obtained from its network. Preliminary investigations showed that modifying the thresholds that designate a node as *influential* led to modest differences in the results and trends. The lack of a gold-standard

solution in determining such a threshold algorithmically remains a key modeling constraint and merits further statistical investigation in future work. Classical approaches like cross-validation do not lend themselves to parameter selection due to the structure of the graph and the inability to break the network into folds. Model improvements that better mimic the spread of disease account for vaccinations, testing, or exposure [32–34].

Each of the novel augmented tracing strategies discussed in this work adds a complexion to one of the existing strategies by leveraging information on node influence in a network. While we present three options that form candidates to replace the existing strategies, there isn't an exhaustive list of strategies that can be engineered. Studying the process of engineering such strategies, particularly based on the specific needs of a situation, coupled with analyzing their efficacies, represents an open area of research. Furthermore, while these novel strategies are evaluated in simulations, the current climate prevents the practical implementations of these strategies due to limitations in human and technical ability to trace contacts between individuals effectively. While challenging in the current climate, the documentation of the efficacies of such strategies can contribute to their implementation in future contexts.

Real-world social association data is sparse and contains substantial uncertainty. Link prediction techniques that can identify potential hidden connections [35,36] can yield substantial progress in emulating the dynamics of real-world networks. In this study, static networks that only account for the presence of social associations are leveraged to demonstrate the feasibility and efficacy of node prioritization-guided novel augmented tracing. In contrast, real-world social links are dynamic in nature, evolve over time, and yield social interactions of varying magnitudes in time and proximity. Studying augmented tracing strategies deployed on epidemics on evolving networks [8] forms a key expanse to explore further. Metadata such as duration and intensity of contacts contribute to inferring contagion dynamics [37]. Firth et al. [6] use weights based on social link strength in their analysis of SARS-CoV-2 on the Haslemere Network. Including metadata in either computing the influence of nodes or simulating the transmission of infection may improve outcomes. In this work, we leverage network structure to aid targeted tracing of nodes. However, network structure can be leveraged to assist targeted adoption of other technical advancements such as by targeting certain influential nodes in a network to deploy technology that can assist with tracing, thereby effectively capturing outbreak dynamics and spread [38]. Leveraging such alternative uses of node influence and the technological advancements available to epidemiology, either independently, or in conjunction with augmented tracing strategies to enhance their efficacy also forms a vital direction to explore for the future. Furthermore, in this study, we observe the efficacy of the novel augmented tracing strategies on networks with undirected edges. In this context, social associations model the possibility of infection transmission between individuals sharing a proximal physical space. However, in certain instances, disease transmission can be directional [28,39,40]. The efficacy of the tracing strategies discussed in this study on networks with directional edges contributes to a key direction for future exploration. Notably, the PRINCE algorithm used for priority scoring is amendable to both directed and signed and directed networks, thereby supporting the feasibility of the adaptation.

Contact tracing, a key non-pharmaceutical intervention in outbreak control, is accompanied by its myriad limitations - key amongst which is the disruption it can cause to society and its participants. When used in its most effective form as secondary tracing, a vast proportion of the population in consideration is placed in quarantine at the same point in time, thereby halting routine functioning. Furthermore, in all forms of contact tracing, psychological tensors and a general sense of uncertainty regarding the path to normal livelihood yield obstacles with compliance. In this work, through the augmentation of existing tracing

strategies, we demonstrate viable alternatives that balance societal disruption due to quarantines while maintaining outbreak control. These strategies, coupled with public health education leading to apt compliance, help mitigate an outbreak's devastating effects on society and individuals.

Supporting information

S1 Fig. Effect of tracing strategies on concurrent quarantines on Barabasi-Albert Preferential Attachment Networks with 1000 nodes and 3990 edges. Concurrent mean isolations, infections, and quarantines with percentile ribbons from outbreak simulations on organized as rows. Columns represent tracing strategies implemented: (A) Primary, (B) Secondary, (C) Selective primary tracing, (D) Selective secondary, and (E) Pseudo-secondary tracing. Solid lines depict mean values, with the shaded ribbons depicting the values observed at the 25th and 75th percentiles.
(PDF)

S2 Fig. A comparison of the effect of tracing strategies on concurrent quarantines when nodes corresponding to the top 20% of PRINCE scores in a network are considered influential. Concurrent mean isolations, infections, and quarantines with percentile ribbons from outbreak simulations on (A) Erdos-Renyi, (B) Barabasi-Albert, and (C) Haslemere Networks, organized as rows. Columns represent tracing strategies implemented: (A1–C1) Primary, (A2–C2) Secondary, (A3–C3) Selective primary tracing, (A4–C4) Selective secondary, and (A5–C5) Pseudo-secondary tracing. Solid lines depict mean values, with the shaded ribbons depicting the values observed at the 25th and 75th percentiles.
(PDF)

S3 Fig. A comparison of the effect of tracing strategies on concurrent quarantines when nodes corresponding to the top 10% of PRINCE scores in a network are considered influential. Concurrent mean isolations, infections, and quarantines with percentile ribbons from outbreak simulations on (A) Erdos-Renyi, (B) Barabasi-Albert, and (C) Haslemere Networks, organized as rows. Columns represent tracing strategies implemented: (A1–C1) Primary, (A2–C2) Secondary, (A3–C3) Selective primary tracing, (A4–C4) Selective secondary, and (A5–C5) Pseudo-secondary tracing. Solid lines depict mean values, with the shaded ribbons depicting the values observed at the 25th and 75th percentiles.
(PDF)

S1 Table.Parameters used with the COVIDHM package.
(PDF)

S2 Table. Cumulative median and mean (with 95% confidence intervals) of isolations, quarantines, and infections across simulations on Barabasi-Albert Preferential Attachment Networks with 1000 Nodes and 3990 edges grouped by intervention strategy.
(PDF)

Author contributions

Conceptualization: Rachael Hageman Blair.

Formal analysis: Adithya Narayanan.

Funding acquisition: Rachael Hageman Blair.

Investigation: Adithya Narayanan, Sarah Muldoon, Matthew Jehrio, Rachael Hageman Blair.

Methodology: Adithya Narayanan, Sarah Muldoon, Matthew Jehrio, Rachael Hageman Blair.

Resources: Rachael Hageman Blair.

Software: Adithya Narayanan.

Visualization: Adithya Narayanan, Rachael Hageman Blair.

Writing – original draft: Adithya Narayanan, Sarah Muldoon, Matthew Jehrio, Rachael Hageman Blair.

Writing – review & editing: Adithya Narayanan, Rachael Hageman Blair.

References

1. Peak CM, Childs LM, Grad YH, Buckee CO. Comparing nonpharmaceutical interventions for containing emerging epidemics. Proc Natl Acad Sci U S A. 2017;114(15):4023–8. https://doi.org/10.1073/pnas.1616438114 PMID: 28351976
2. Chatterjee K, Chauhan VS. Epidemics, quarantine and mental health. Med J Armed Forces India. 2020;76(2):125–7. https://doi.org/10.1016/j.mjafi.2020.03.017 PMID: 32327877
3. Tseng C-W, Roh Y, DeJong C, Kanagusuku LN, Soin KS. Patients' compliance with quarantine requirements for exposure or potential symptoms of COVID-19. Hawaii J Health Soc Welf. 2021;80(11):276–82. PMID: 34765987
4. DiGiovanni C, Conley J, Chiu D, Zaborski J. Factors influencing compliance with quarantine in Toronto during the 2003 SARS outbreak. Biosecur Bioterror. 2004;2(4):265–72. https://doi.org/10.1089/bsp.2004.2.265 PMID: 15650436
5. Danon L, Ford AP, House T, Jewell CP, Keeling MJ, Roberts GO, et al. Networks and the epidemiology of infectious disease. Interdiscip Perspect Infect Dis. 2011;2011:284909. https://doi.org/10.1155/2011/284909 PMID: 21437001
6. Firth JA, Hellewell J, Klepac P, Kissler S, CMMID COVID-19 Working Group, Kucharski AJ, et al. Using a real-world network to model localized COVID-19 control strategies. Nat Med. 2020;26(10):1616–22. https://doi.org/10.1038/s41591-020-1036-8 PMID: 32770169
7. Bisset KR, Feng X, Marathe M, Yardi S. Modeling interaction between individuals, social networks and public policy to support public health epidemiology. In: Proceedings of the 2009 Winter Simulation Conference (WSC). IEEE. 2009. 2020–31. https://doi.org/10.1109/wsc.2009.5429672
8. Sanhedrai H, Havlin S. Epidemics on evolving networks with varying degrees. New J Phys. 2022;24(5):053002. https://doi.org/10.1088/1367-2630/ac64b8
9. Teicher A. Super-spreaders: a historical review. Lancet Infect Dis. 2023;23(10):e409–17. https://doi.org/10.1016/S1473-3099(23)00183-4 PMID: 37352877
10. Rambo APS, Gonçalves LF, Gonzáles AI, Rech CR, Paiva KM de, Haas P. Impact of super-spreaders on COVID-19: systematic review. Sao Paulo Med J. 2021;139(2):163–9. https://doi.org/10.1590/1516-3180.2020.0618.R1.10122020 PMID: 33605305
11. Lin J, Yan K, Zhang J, Cai T, Zheng J. A super-spreader of COVID-19 in Ningbo city in China. J Infect Public Health. 2020;13(7):935–7. https://doi.org/10.1016/j.jiph.2020.05.023 PMID: 32554034
12. Vanunu O, Magger O, Ruppin E, Shlomi T, Sharan R. Associating genes and protein complexes with disease via network propagation. PLoS Comput Biol. 2010;6(1):e1000641. https://doi.org/10.1371/journal.pcbi.1000641 PMID: 20090828
13. Albert R, Jeong H, Barabasi A. Error and attack tolerance of complex networks. Nature. 2000;406(6794):378–82. https://doi.org/10.1038/35019019 PMID: 10935628
14. Hansen D, Shneiderman B, Smith MA. Analyzing social media networks with NodeXL: insights from a connected world. Morgan Kaufmann. 2010.
15. Freeman LC. Centrality in social networks conceptual clarification. Social Networks. 1978;1(3):215–39. https://doi.org/10.1016/0378-8733(78)90021-7
16. Chen D-B, Gao H, Lü L, Zhou T. Identifying influential nodes in large-scale directed networks: the role of clustering. PLoS One. 2013;8(10):e77455. https://doi.org/10.1371/journal.pone.0077455 PMID: 24204833
17. Zhou D, Bousquet O, Lal T, Weston J, Schölkopf B. Learning with local and global consistency. In: Adv Neural Inf Process Syst. 2003.
18. Csardi G, Nepusz T. The igraph software package for complex network research. Int J Complex Syst. 2006;1695(5):1–9.

19. Erdős P, Rényi A. On random graphs. I. Publicationes Mathematicae Debrecen. 1959;6:290–7.
20. Barabasi A, Albert R. Emergence of scaling in random networks. Science. 1999;286(5439):509–12. https://doi.org/10.1126/science.286.5439.509 PMID: 10521342
21. Kissler SM, Klepac P, Tang M, Conlan AJ, Gog JR. Sparking the BBC Four pandemic: leveraging citizen science and mobile phones to model the spread of disease. bioRxiv. 2020. p. 479154.
22. Hellewell J, Abbott S, Gimma A, Bosse NI, Jarvis CI, Russell TW, et al. Feasibility of controlling COVID-19 outbreaks by isolation of cases and contacts. Lancet Glob Health. 2020;8(4):e488–96. https://doi.org/10.1016/S2214-109X(20)30074-7 PMID: 32119825
23. Yang Y, Xie G. Efficient identification of node importance in social networks. Inf Process Manag. 2016;52(5):911–22. https://doi.org/10.1016/j.ipm.2016.04.001
24. Beni HA, Bouyer A. TI-SC: top-k influential nodes selection based on community detection and scoring criteria in social networks. J Ambient Intell Human Comput. 2020;11(11):4889–908. https://doi.org/10.1007/s12652-020-01760-2
25. Wei X, Zhao J, Liu S, Wang Y. Identifying influential spreaders in complex networks for disease spread and control. Sci Rep. 2022;12(1):5550. https://doi.org/10.1038/s41598-022-09341-3 PMID: 35365715
26. Bucur D, Holme P. Beyond ranking nodes: Predicting epidemic outbreak sizes by network centralities. PLoS Comput Biol. 2020;16(7):e1008052. https://doi.org/10.1371/journal.pcbi.1008052 PMID: 32697781
27. May RM. Network structure and the biology of populations. Trends Ecol Evol. 2006;21(7):394–9. https://doi.org/10.1016/j.tree.2006.03.013 PMID: 16815438
28. Silk MJ, Croft DP, Delahay RJ, Hodgson DJ, Boots M, Weber N, et al. Using social network measures in wildlife disease ecology, epidemiology, and management. Bioscience. 2017;67(3):245–57. https://doi.org/10.1093/biosci/biw175 PMID: 28596616
29. Yu P-D, Tan CW, Fu H-L. Epidemic source detection in contact tracing networks: epidemic centrality in graphs and message-passing algorithms. IEEE J Sel Top Signal Process. 2022;16(2):234–49. https://doi.org/10.1109/jstsp.2022.3153168
30. Doostmohammadian M, Rabiee HR, Khan UA. Centrality-based epidemic control in complex social networks. Soc Netw Anal Min. 2020;10(1):1–11. https://doi.org/10.1007/s13278-020-00638-7
31. Kermack WO, McKendrick AG. A contribution to the mathematical theory of epidemics. Proc R Soc Lond A. 1927;115(772):700–21.
32. Carcione J, Santos J, Bagaini C, Ba J. A simulation of a COVID-19 epidemic based on a deterministic SEIR model. Front Public Health. 2020; 230.
33. Schlickeiser R, Kröger M. Analytical modeling of the temporal evolution of epidemics outbreaks accounting for vaccinations. Physics. 2021;3(2):386–426. https://doi.org/10.3390/physics3020028
34. He S, Peng Y, Sun K. SEIR modeling of the COVID-19 and its dynamics. Nonl Dyn. 2020;101(3):1667–80. https://doi.org/10.1007/s11071-020-05743-y PMID: 32836803
35. Clauset A, Moore C, Newman MEJ. Hierarchical structure and the prediction of missing links in networks. Nature. 2008;453(7191):98–101. https://doi.org/10.1038/nature06830 PMID: 18451861
36. Lim M, Abdullah A, Jhanjhi NZ, Khurram Khan M, Supramaniam M. Link prediction in time-evolving criminal network with deep reinforcement learning technique. IEEE Access. 2019;7:184797–807. https://doi.org/10.1109/access.2019.2958873
37. Smieszek T. A mechanistic model of infection: why duration and intensity of contacts should be included in models of disease spread. Theor Biol Med Model. 2009;6:25. https://doi.org/10.1186/1742-4682-6-25 PMID: 19919678
38. Bassolas A, Santoro A, Sousa S, Rognone S, Nicosia V. Optimizing the mitigation of epidemic spreading through targeted adoption of contact tracing apps. Phys Rev Res. 2022;4(2):023092.
39. Liu R, Shuai J, Wu J, Zhu H. Modeling spatial spread of west nile virus and impact of directional dispersal of birds. Math Biosci Eng. 2006;3(1):145–60. https://doi.org/10.3934/mbe.2006.3.145 PMID: 20361815
40. Meyers LA, Newman MEJ, Pourbohloul B. Predicting epidemics on directed contact networks. J Theor Biol. 2006;240(3):400–18. https://doi.org/10.1016/j.jtbi.2005.10.004 PMID: 16300796